PASSIVITY BREAKDOWN OF TITANIUM IN LiBr SOLUTIONS

Fernández-Domene, R.M., Blasco-Tamarit, E., García-García, D.M., García-Antón, J. *

Ingeniería Electroquímica y Corrosión (IEC). Departamento de Ingeniería Química y Nuclear. ETSI Industriales. Universitat Politècnica de València. Camino de Vera s/n, 46022 Valencia, Spain.

**Corresponding author. Tel. 34-96-387 76 32, Fax. 34-96-387 76 39, e-mail: jgarciaa@iqn.upv.es (J. García-Antón); raferdo1@etsii.upv.es (R.M. Fernández-Domene).*

The passive behavior of titanium and its susceptibility to undergo localized attacks in different LiBr solutions at 25º C have been investigated using different electrochemical techniques: potentiodynamic polarization curves, potentiostatic passivation tests, EIS measurements and Mott-Schottky analysis. In low and moderately concentrated LiBr solutions, the breakdown potential E_b decreased with increasing bromide concentrations, while in highly concentrated LiBr solutions, E_b increased with increasing LiBr concentration. In the most concentrated LiBr solution (11.42M) Ti did not undergo passivity breakdown even at 9 $V_{Ag/AgCl}$. These results have been related to a decrease in the activity of water in highly concentrated LiBr solutions.

Keywords: titanium; passivity breakdown; bromide solutions; activity of water; point defect model.

1. INTRODUCTION

Titanium is a very reactive metal that shows remarkable corrosion resistance in many environments due to the formation of a very stable, continuous, highly adherent, and protective passive oxide film on the metal surface. A freshly abraded titanium surface immediately passivates when exposed to an oxygen source (air and/or moisture). The nature, composition, and thickness of the passive film that forms on titanium depend on the environmental conditions. In most aqueous environments, the oxide is typically TiO_2, but may consist of mixtures of other titanium oxides, including TiO_2, Ti_2O_3, and TiO [1-8]. The oxygen content of the titanium oxide gradually decreases from TiO_2 at the surface, to Ti_2O_3 and TiO as it approaches the metal/oxide interface [1]. Depending on the environment, this oxide may be covered with an amorphous or hydrated surface oxide, giving a two-layer oxide structure [1, 4, 5, 9]. The TiO_2 passive film is an n-type semiconductor and its semiconductive properties determine the current/potential behavior of the titanium/passive film/electrolyte system [1, 6, 10-13]. The metal/passive film interface has been assumed to be an ohmic contact with minimal resistance. On the other hand, a space charge region has been hypothesized to develop at the passive film/electrolyte interface [6]. Oxygen vacancies have been reported to be the main defects within the passive film on titanium [13-15]. Ti^{3+} interstitials have also been cited as electron donor species [10, 12].

Titanium exhibits excellent resistance to most salt solutions over a wide range of pH and temperatures [16]. Although titanium is resistant to these media, it is not immune and can be susceptible to pitting and crevice attack, depending on the environmental conditions [15-18]. Breakdown potentials (E_b) of titanium in sulfate and phosphate

media are typically in excess of 80 V_{SCE} [1, 19]. Values of 5 to 12 V_{SCE} can be expected in room-temperature chloride solutions [1, 15, 18, 19]. However, it has been observed in numerous works that bromide anions are far more effective than chlorides or iodides in facilitating breakdown of the passive film formed on Ti [15, 17-22]. In fact, many authors have observed passivity breakdown of titanium in bromide containing solutions taking place at relatively low potentials compared to those in chloride or iodide containing solutions (E_b < 2-5 V_{SCE}) [15, 17-24]. Sazou et al. [15] interpreted this high susceptibility of TiO_2 to local breakdown in the presence of bromides by considering electrochemical reactions taking place at the passive film/electrolyte interface, such as the formation of surface titanium peroxo-species, leading to changes in the surface and bulk properties (ionic and electronic) of the titanium oxide. The breakdown potential of titanium in relatively low concentrated bromide solutions (up to 1M) has been found to decrease with increasing bromide concentrations [15, 18, 20], with values in the range of 2-5 $V_{Ag/AgCl}$. Nevertheless, it has been observed in recent works [2, 25] that in very concentrated LiBr solutions (700, 850 and 992 g/l LiBr, 8.06M, 9.78M and 11.42, respectively), titanium did not undergo localized attacks at potentials as high as 3$V_{Ag/AgCl}$. These results contradict the tendencies found in the literature for E_b with bromide concentration, since in heavy brine LiBr solutions the values of E_b should be lower than 2-3 $V_{Ag/AgCl}$.

The aim of the present work is to study the influence of bromide concentration on the passivity breakdown of titanium at 25º C and to clarify the anomalous behavior of passive films formed on titanium in highly concentrated LiBr solutions against localized attacks. These heavy brine LiBr solutions are widely used in absorption cooling systems [26-30]. The steady-state properties of the passive film formed on Ti electrodes in

different LiBr solutions have been studied in this work, as well as the role of electronic properties and the activity of water on the stability of Ti passive film.

2. MATERIALS AND METHODS

Materials, solution and electrochemical cell

The material tested was commercially pure Grade 2 titanium (0.03 wt.% N, 0.1 wt.% C, 0.25 wt.% O, 0.3 wt.% Fe, 0.0125 wt.% H, Bal. Ti). Titanium electrodes were cylindrically shaped and covered with a polytetrafluoroethylene (PTFE) coating, to expose an area of 0.5 cm^2 to the test solution. All specimens were wet abraded from 200 to 4000 SiC grit, and finally rinsed with distilled water and air-dried. Titanium electrodes were tested in different LiBr solutions, from 0.05M to 11.42M, at a constant temperature of 25º C (**Table 1**). Values of molalities (m_{LiBr}), mean ionic activity coefficients ($\gamma_{\pm}$), activities of LiBr solutions (a_{LiBr}), osmotic coefficients (ϕ) and activities of water (a_W) are also shown in **Table 1**. Activities for LiBr solutions, a_{LiBr}, have been calculated from the following equation:

$$a_{LiBr} = \frac{m_{LiBr}}{m^0}\gamma_{\pm} \quad \textbf{(1)}$$

where the LiBr molality, m_{LiBr}, is defined as mol LiBr/kg H_2O and m^0 is the standard LiBr molality (m^0 = 1 mol LiBr/kg H_2O). Activity coefficients and osmotic coefficients have been obtained from the literature [31]. Activities of water have been calculated from osmotic coefficients according to the following expression [32, 33]:

$$\ln(a_W) = -\phi M_W \nu m \quad \textbf{(2)}$$

where M_W is the molar mass of water and ν is the stoichiometric parameter, i.e., the number of ion moles produced by complete dissociation of one mole of salt (for a 1:1 salt such as LiBr, ν equals 2); notice that molality m is expressed in kilomole of solute per kilogram of solvent (or mole of solute per gram of solvent) so the units in eq. (2) are consistent.

To study the effect of solvent nature and the influence of the bromide salt on the passivity breakdown of Ti, additional experiments were carried out in different electrolytes: 0.5M LiBr solutions with different water-methanol proportions (70 mol%, 50 mol% and 0 mol% water), and a 3M KBr solution.

The electrochemical tests were performed in a sheathed vertical electrochemical cell. A silver-silver chloride (Ag/AgCl 3M KCl) was used as reference electrode and a platinum wire as auxiliary electrode. Electrochemical measurements were performed using an Autolab PGSTAT302N potentiostat. In all cases the tests were repeated at least three times in order to verify reproducibility.

Potentiodynamic polarization curves

Polarization tests began at a cathodic potential value of -0.9 $V_{Ag/AgCl}$ and the potential was subsequently scanned anodically at a scan rate of 0.5 mV s^{-1}. The passive current density, i_p, and the breakdown potential, E_b (defined as the potential at which the current density increases abruptly after the peak corresponding to the Br^-/Br_2 oxidation), were

obtained from potentiodynamic polarization tests. After potentiodynamic polarization, the morphological inspection of the Ti electrodes surface was done using a Leica DM LA optical microscope.

Potentiostatic passivation tests

Before the potentiostatic passivation experiments, the surface of the Ti electrodes was pretreated cathodically at -0.9 $V_{Ag/AgCl}$ for 30 min to create reproducible initial conditions. Afterwards, the working electrode was polarized at a potential within the passive region of titanium (0.4 $V_{Ag/AgCl}$) for 1 hour in several LiBr solutions (0.1M, 0.5M, 3M and 11.42M) at 25º C, to form a stable passive film. During passivation experiments, transients in the current density were recorded against time.

EIS and capacitance measurements

EIS and capacitance measurements were performed under potentiostatic conditions after the passivation tests, once a stable passive film was formed on the surface of the Ti samples. EIS measurements were conducted using a sinusoidal signal of 10 mV in amplitude in the frequency range of 100 kHz-10 mHz. Capacitance measurements were performed at a frequency of 10 kHz applying a sinusoidal potential perturbation of 10 mV and scanning the potential from the formation value in the negative direction at a rate of 25 mV s^{-1}.

3. RESULTS AND DISCUSSION

Potentiodynamic polarization curves

The potentiodynamic polarization curves obtained for Ti in different LiBr solutions at 25º C are shown in **Figure 1**. A wide passive range can be observed in all LiBr solutions where passive current density values (i_p) remain very low (of the order of 1-3 μA cm^{-2}), indicating the excellent passive behavior of Ti (**Table 2**). The values of i_p have been estimated at a potential of 0.4 V, within the stable passive region. At first, i_p slightly increases with increasing LiBr concentrations, but at concentrations higher than 0.7 M it starts decreasing until reaching its lowest value (1 μA cm^{-2}) in the 11.42 LiBr solution.

Upon increasing the anodic polarization of Ti, the occurrence of a broad anodic wave can be observed at potentials between 1-1.5 V, corresponding to the oxidation of bromides present in the solution ($E^0(Br_2/Br^-)$ = 0.89 $V_{Ag/AgCl}$). This anodic wave is more evident at high LiBr concentrations. In fact, in the potential range between 1-1.5 V a change of the solution color around the titanium electrode surface (from colorless to yellow-orange) was noticeable at high LiBr concentrations. This change in color is related to the localized oxidation of bromide ions to bromine (Br_2) at electroactive sites at potentials around 1.5 $V_{Ag/AgCl}$ [15, 17-20, 22] and to the subsequent formation of HBrO, according to the following equations [34]:

$$2Br^- \Leftrightarrow Br_2 + 2e^- \quad \textbf{(3a)}$$

$$Br_2 + H_2O \rightarrow HBrO + Br^- + H^+ \quad \textbf{(3b)}$$

Apart from the oxidation of Br^-, several processes may take place simultaneously during anodic polarization of titanium at high potentials, such as oxygen evolution reaction (OER) [2, 19, 21, 23, 25, 35], oxidation of TiO and Ti_2O_3 to TiO_2 [2, 3, 5, 25, 35] or additional oxidation of TiO_2 to form soluble complex species, such as TiO^{2+} [36], or/and peroxo-species, such as TiO_3 or TiOOH [7, 8, 10, 15].

The abrupt increase of current density at potentials above the Br^- oxidation peak indicates the onset of passivity breakdown of Ti. Once exposed to the Br^- solution, the Ti metal rapidly oxidizes to a soluble oxi-halide Ti^{4+} species [18, 23]. In the low and moderately concentrated LiBr solutions (**Figure 1a**) a decrease of E_b with increasing bromide concentration can be observed, as reported in the literature [15, 18, 20] (**Table 2**). In the more concentrated LiBr solutions (**Figure 1b**), on the other hand, E_b does not follow the previous tendency, since its value increases with increasing LiBr concentration (**Table 2**). In fact, in the 11.42M LiBr solution Ti did not undergo localized attacks under the experimental conditions (up to 9 $V_{Ag/AgCl}$), indicating that E_b is apparently higher than 9 $V_{Ag/AgCl}$, which is a behavior more typical of chloride- or iodide- than bromide-containing solutions [18]. A similar behavior was observed by Davydov for niobium in LiBr solutions [37]. By way of illustration, **Figure 2** shows the images of the Ti electrode surface before and after the polarization tests in 0.5M (**Figure 2a**) and 11.42M (**Figure 2b**) LiBr solution. Visual inspection of the Ti electrode polarized in the 0.5M LiBr solution (**Figure 2a**) reveals the presence of several large corrosion pits. On the other hand, no damage is observed on the Ti electrode polarized in the 11.42M LiBr solution up to 9 V (**Figure 2b**), in accordance with the description of the polarization curves made above.

Figure 3 shows the plot of E_b vs. the logarithm of bromide activity (log a_{Br^-}) for all the LiBr solutions under study. It can be observed that E_b decreases linearly with log a_{Br^-} for the low and moderately concentrated LiBr solutions, while it increases linearly with log a_{Br^-} for the highly concentrated LiBr solutions (except in the 11.42M LiBr solution, where passivity breakdown was not observed at all under the experimental conditions, as commented above). The linear relationship with negative slope between E_b and log a_{Br^-} (in low and moderately concentrated LiBr solutions) has been predicted analytically by the Point Defect Model (PDM) [38, 39], according to the following equation:

$$E_b = \left(\frac{4.606RT}{\chi\alpha F}\right)\log\left(\frac{b}{D}\right) - \frac{2.303RT}{\alpha F}\log\left(a_{Br^-}\right) \quad \textbf{(4)}$$

where χ is the charge of the metal ions (Ti^{4+}), α is the polarizability of the passive film/solution interface, F is Faraday's constant (96485.34 C mol^{-1}), b is a constant, D is the diffusivity of cation vacancies in the passive film, R is the gas constant and T is absolute temperature. From the straight line with negative slope shown in **Figure 3**, the value of α can be determined, yielding a value of 0.045. This low value is comparable to those reported in the literature for Ti [13, 15]. A low value of α suggests that the Helmholtz layer is very weakly polarized since the potential drop at the passive film/solution interface is negligible. Thus, almost all the potential drop in the interfacial regions takes place in the metal/passive film interface, where the reaction of passive film formation and growth occurs according to the PDM [40-42].

Potentiostatic passivation tests

The current density transients obtained after applying a potential step from a value of -0.9 V (cathodic pre-treatment) to a value of 0.4 V within the passive region are shown in **Figure 4** for different LiBr solutions (0.1M, 0.5M, 3M and 11.42M). It can be observed that current densities follow the same tendency as i_p, that is, the order from highest to lowest values during the whole potentiostatic test is: 0.5M, 3M, 0.1M and 11.43 LiBr solutions. In all cases, current density values decrease exponentially with passivation, and eventually reach a steady-state value (i_{SS}). These values are the following: 0.12±0.05 μA cm^{-2} (0.1M), 0.22±0.07 μA cm^{-2} (0.5M), 0.17±0.05 μA cm^{-2} (3M) and 0.059±0.03 μA cm^{-2} (11.42M). Virtanen and Curty [20] observed a clear increase in passive current density with increasing bromide concentrations for Ti in NaBr. However, in the present study, i_{SS} increases with Br^- concentration at relatively low concentrations, but it decreases with concentration at high LiBr concentrations.

According to the PDM [42-44], the steady-state current density can be written as:

$$i_{SS} = \delta F\left[k_{\text{int}} + k_{cat} + k_{dis}\left(\frac{C_{H^+}}{C^0_{H^+}}\right)^n\right] \quad \textbf{(5)}$$

where δ is the charge of the cation ejected from the passive film (3 in the case of Cr^{3+}), C_{H^+} is the proton concentration in the solution, $C^0_{H^+}$ is a standard state H^+ concentration and n is the kinetic order of the reaction of passive film dissolution with respect to $\left(C_{H^+}/C^0_{H^+}\right)$. The parameters k_{int}, k_{cat} and k_{dis} are the rate coefficients for the reactions of formation of cation interstitials, cation vacancies and of passive film dissolution, respectively. Eq. (5) suggests that the steady-state current density i_{SS} is associated with the fluxes of point defects and also with the kinetic parameters for the interfacial

reactions. Hence, i_{SS} consists of three components: the first ($\delta F k_{int}$) resulting from the generation and transport of cation interstitials, the second ($\delta F k_{cat}$) resulting from the generation and transport of cation vacancies and the third $\delta F k_{dis}\left(C_{H^+}/C^0_{H^+}\right)^n$ resulting from the movement of oxygen vacancies. The latter term is expressed in terms of the dissolution rate of the passive film [42-45].

The passive film on titanium is well known to behave as an *n*-type semiconductor [1, 6, 10-13] (see Mott-Schottky analysis below), whose donor species are oxygen vacancies and/or Ti^{3+} interstitials [10, 12-15], so the term related to the generation and transport of cation vacancies, k_{cat}, can be neglected [43]. Therefore, the differences between current densities with LiBr concentration are either due to the process of generation and transport of cation interstitials or the dissolution of the passive film closely related to the generation and movement of oxygen vacancies in the steady-state [41].

Mott-Schottky analysis

In order to check if the differences observed in i_{SS} at different LiBr concentrations is due to the generation of donor species at the metal/passive film interface (oxygen vacancies and/or cation interstitials), the electrochemical capacitance of the passive system was measured as a function of the applied potential. Mott-Schottky (M-S) analysis was performed to obtain the donor density, N_D, of the passive films formed on Ti in different LiBr solutions. The total capacitance has been calculated from the imaginary component of the impedance (Z'') using the relationship $C = -1/\omega Z''$, where ω is the angular frequency.

As an illustration, **Figure 5** shows the capacitance-potential curves obtained for Ti in the 0.5M LiBr solution at 0.4 V and at different frequencies. It is clearly observed that capacitance values depend strongly on frequency. Capacitance-potential curves shift to lower values with increasing frequencies. Such behavior has been frequently observed for semiconducting passive films formed on metals and alloys [12, 46-54]. Several physical explanations have been suggested in the literature as possible sources of this dependence [46-54], such as the presence of deep donor states, contribution of surface states, surface roughness, ionic charges movement, frequency dependant dielectric constant, etc. It can be seen from **Figure 5** that capacitance becomes almost independent of frequency at approximately 10 kHz. Therefore, a value of 10 kHz has been used in this work to eliminate capacitance dependence on frequency.

Figure 6 shows the Mott-Schottky plots at a frequency of 10 kHz of the passive film formed on Ti in 0.1M, 0.5M, 3M and 11.42M LiBr solutions at 0.4 V. The positive slopes of the M-S plots are characteristic of *n*-type semiconductors, with the dominant defects in the passive film being oxygen vacancies and/or Ti^{3+} interstitials, as it has been mentioned above.

The donor density, N_D, can be determined from the slopes in the M-S plots, according to the following equation [10, 12]:

$$N_D = \frac{2}{\varepsilon \varepsilon_0 e \sigma} \qquad \textbf{(6)}$$

where ε is the dielectric constant of the passive film (a value of 60 has been assumed for the passive film formed on Ti [15]), ε_0 is the vacuum permittivity ($8.85 \cdot 10^{-14}$ F/cm), e is

302 the electron charge ($1.60 \cdot 10^{-19}$ C) and σ is the positive slope of each straight line in the
303 M-S plots.
304
305 The values of N_D are presented in **Figure 7** for different LiBr solutions (0.1M, 0.5M,
306 3M and 11.42M) at 0.4 V. The results show that N_D values are of the order of 10^{19}-10^{20}
307 cm^{-3}, regardless the LiBr concentration, which is in agreement with those reported in the
308 literature for TiO_2 [10, 12].
309
310 An increase in LiBr concentration from 0.1M to 0.5M leads to a clear increase of N_D
311 (**Figure 7**). The PDM [38, 40, 55] assumes that the initial event that takes place at the
312 passive film/electrolyte interface in passivity breakdown is the occupation of surface
313 oxygen vacancies by aggressive anions, such as bromides:
314
315 $$V_O^{\bullet\bullet} + \mathrm{Br}^- \rightarrow \mathrm{Br}_\mathrm{O}^{\bullet} \quad \textbf{(7)}$$
316
317 where $\mathrm{Br}_\mathrm{O}^{\bullet}$ represents a bromide anion adsorbed into an oxygen vacancy, $V_O^{\bullet\bullet}$, in the
318 film/electrolyte interface. This process is followed by a Schottky-pair type reaction:
319
320 $$\mathrm{Null} \rightarrow V_{Ti}^{4'} + \left(\frac{\chi}{2}\right) V_O^{\bullet\bullet} \quad \textbf{(8)}$$
321
322 where V_{Ti}^4 is a cation vacancy in the Ti passive film. Kroger-Vink notation is used for
323 the effective positive ($^{\bullet\bullet}$) and negative ($^{4'}$) charges in oxygen and cation vacancies,
324 respectively.
325

The adsorbed Br^- anions could desorb along with a surface cation to form a cation vacancy/oxygen vacancy pair $(V_{Ti}^{4'} V_O^{\bullet\bullet})^{2'}$. This pair is subsequently annihilated, leading to the formation of a subsurface cation vacancy and the regeneration of the surface $V_O^{\bullet\bullet}$:

$$\left(V_{Ti}^{4'} V_O^{\bullet\bullet}\right)'' \rightarrow \left(V_{Ti}^{4'}\right)_S + V_O^{\bullet\bullet} \quad \textbf{(9)}$$

where the subscript *S* indicates a subsurface position in the passive film. The oxygen vacancies continue reacting with additional Br^- at the film/electrolyte interface to generate additional cation and oxygen vacancies. Hence, the generation of cation and oxygen vacancies through eqs. (7)-(9) is autocatalytic.

Anion adsorption leads to the generation of cation vacancies at the film/solution interface and hence to an enhancement in the flux of cation vacancies across the passive film to the film/metal interface due to the outward movement (towards the passive film/electrolyte interface) of cations in the film. If the flux of cation vacancies exceeds the rate at which they are annihilated at the metal/film interface, the excess vacancies will condense at the interface and the passive film will be locally detached from the metal. As passive film dissolution continues, the film thins locally, eventually leading to film breakdown [40].

According to the previous explanation, since oxygen vacancies are donor species, the higher the donor density in the passive film, N_D, the lower the resistance to passivity breakdown. This affirmation is in agreement with the values of the breakdown potential, E_b, shown in **Table 2**, where $E_{b0.5M} < E_{b0.1M}$. However, when increasing the LiBr concentration from 0.5M to 3M and 11.42M, N_D decreases, indicating that the higher

bromide concentration in the 3M and 11.42M LiBr solutions does not lead to a higher degree of oxygen vacancies occupation by bromide ions. This result could explain the lower susceptibility of Ti to undergo passivity breakdown in the 3M and 11.42M LiBr solutions if compared with the 0.5M LiBr solution. Nevertheless, since the N_D values obtained in concentrated LiBr solutions are still higher than that in the 0.1M LiBr solution, this fact cannot satisfactorily explain the increase of E_b at high LiBr concentrations or even the absence of passivity breakdown in the 11.42M LiBr solution.

The tendency of N_D with LiBr concentration also confirms that the differences mentioned above in the steady-state current density (i_{SS}) with LiBr concentration are not related to the density of donor species (oxygen vacancies and/or cation interstitials), since $i_{SS0.1M} > i_{SS11.42M}$ but $N_{D0.1M} < N_{D11.42M}$.

EIS measurements

Mott-Schottky analysis has proved that the behavior of the passive film on Ti against localized attacks in high LiBr concentrations is not directly related with its electronic properties. **Figure 8** shows the experimental and simulated Nyquist diagrams for Ti in 0.1M, 0.5M, 3M and 11.42M LiBr solutions at 0.4 V. The experimental data have been fitted to the electrical equivalent circuit shown in **Figure 9**, commonly used to account for the bilayer structure of the passive film on Ti (porous outer layer and compact inner layer) [4, 5, 56]

In all cases, Nyquist plots exhibit a typical passive state behavior characterized by semicircular shape and high impedance values, suggesting that a highly stable film is formed on all the electrodes [31-34].

An increase in LiBr concentration from 0.1M to 0.5M reduces the amplitude of the semicircle in Nyquist plots, indicating a decrease of the total impedance of the system and a loss in the protective properties of the passive film. This result is consistent with the higher i_{SS} and N_D values obtained in the 0.5M LiBr solution. However, upon increasing the bromide concentration to 3M and 11.42M, the total impedance increases again, which agrees with the tendency of i_{SS} observed before (the lower the i_{SS}, the higher the total impedance of the system), but differs in the case of N_D values (**Figure 7**), since the lowest N_D value (0.1M LiBr solution) does not imply the highest impedance values.

The values of the equivalent circuit parameters are shown in **Table 3**. In this equivalent circuit, R_S represents the solution resistance, the time constant at high frequencies (R_1CPE_1) is related to the outer layer of the passive film (hydroxides), whereas the low-frequency behavior (R_2CPE_2) is attributed to the inner layer (mainly TiO_2), more compact than the outer one. Constant Phase Elements (CPEs) have been used instead of pure capacitors, to describe the non-ideality of the system studied. CPEs have been converted into pure capacitance, C, by using the following equation [57, 58]:

$$C = \frac{(Q \cdot R)^{1/\alpha}}{R} \qquad \textbf{(10)}$$

where Q is the impedance of the CPE and R corresponds to R_2 when determining capacitance values of the second time constant in **Figure 9**. To determine C_1 from CPE_1, R has been calculated as follows:

$$\frac{1}{R} = \frac{1}{R_S} + \frac{1}{R_1} \quad \textbf{(11)}$$

It can be observed from **Table 3** that the resistance values of the compact inner layer (R_2) are significantly larger than the values associated with the outer porous layer (R_1), which is consistent with the chosen physical model. These results indicate that the protection provided by the passive film is predominantly due to the barrier layer. In general, both the outer and inner layers exhibit similar capacitance values, of the order of some μF cm^{-2}. Regarding the influence of LiBr concentration on the parameters, it can be observed that R_1 decreases at high LiBr concentrations, while R_2 decreases from 0.1M to 0.5M but then it increases again, reaching the highest value in the 11.42M LiBr solution. These results are in agreement with those obtained for i_{SS} (the lower the value of i_{SS}, the higher the resistance of the barrier inner layer of the passive film, R_2).

According to the M-S results, the increase of R_2 in the 3M and 11.42M LiBr solutions with respect to the value in the 0.1M LiBr solution cannot be related to the degree of defectiveness of the passive film on Ti (**Figure 7 and Table 3**). This increase of R_2 could be explained in terms of the passive film dissolution and the influence of the activity of water, a_W, on this process. Water is one of the reacting species in electrochemical and corrosion mechanisms, but most corrosion works focus on the properties of solutes whereas changes in the activity of water are rarely considered [33, 59]. Smart and Bockris [59] observed a decrease in the corrosion current density of iron in concentrated chloride media with decreasing free water in the solution, that is, the

rate of iron dissolution (Fe/Fe^{2+}) was shown to strongly decrease with decreasing activity of water. Hence, in the case of Ti in highly concentrated LiBr solution, the decrease of a_W (**Table 1**) might lead to similar results. The reaction of dissolution of the passive film formed on Ti by proton attack can be expressed as follows:

$$TiO_2 + 4H^+ \rightarrow Ti^{4+}_{aq} + 2H_2O \quad \textbf{(12)}$$

Although the activity of protons, a_{H+}, is constant, the concentration of H^+ will decrease with decreasing free water (decreasing a_W). Therefore, the dissolution reaction given by eq. (12) not only depends on pH (a_{H+}) but also on the number on H^+ at the passive film/electrolyte interface, which in turn depends on a_W. Passive film dissolution is a necessary step for passivity breakdown to occur, causing the thinning and subsequent rupture of the passive film [40, 60]. Therefore, if passive film dissolution is somehow hampered, for example by reducing the activity of water, passivity breakdown will appear at higher potentials. This fact would explain the increase of E_b in highly concentrated LiBr solutions (**Table 2**).

On the other hand, the formation of the precipitated outer layer ($TiO_2 \cdot nH_2O$) via the hydrolysis of Ti^{4+} cations ejected from the inner layer (eq. (12)) also depends on a_W:

$$Ti^{4+}_{aq} + (n+2)H_2O \rightarrow TiO_2 \cdot nH_2O + 4H^+ \quad \textbf{(13)}$$

In fact, the values of the outer layer resistance, R_1, are higher in the 0.1M and 0.5M LiBr solutions (**Figure 7**), indicating that the formation of precipitated hydroxides is favored when a_W values are close to unity (**Table 1**).

However, the explanations given above concerning the dissolution of the passive film do not completely explain why this behavior has not been observed, for example, in stainless steels in highly concentrated LiBr solutions [35, 61, 62]. Apart from the process of passive film dissolution (eq. (12)), there must be other Ti-specific surface processes which are influenced by the decrease of a_W in highly concentrated LiBr solutions. Davydov [37] suggested that the formation of an intermediate complex between a valve metal (such as Ti) and the aggressive anions (Br^-) and its interaction with the metal oxide could restrict the process of metal dissolution. Following the descriptions of Davydov [37], this complex is formed when a bromide anion adsorbs on a surface oxygen vacancy (eq. (7)) and then interacts with a Ti cation in the passive film (Ti_{Ti}), according to the following reaction:

$$Ti_{Ti} + aBr_O^{\bullet} \rightarrow \left[TiBr_a^z\right]_s + ne^- \qquad \textbf{(14)}$$

where $z = n + a$ and $\left[TiBr_a^z\right]_s$ is the surface complex. Along with the complex formation, a cation vacancy/anion vacancy pair is also generated via a Schottky-pair type reaction, eq. (8). The hydrolysis of the complex will break the bond with the passive film, thus favoring the process of dissolution with the formation of the product of activated dissolution, $TiO_2{\cdot}nH_2O$:

$$2\left[TiBr_a^z\right]_s + (5+n)H_2O \rightarrow TiO_2{\cdot}nH_2O + 2aBr^- + 10H^+ \qquad \textbf{(15)}$$

As in the case of eq. (12), a decrease in the content of free water (i.e. decrease in a_W) will slow down the process of hydrolysis and, as a consequence, the full process of passivity breakdown.

474

475 **Influence of solvent and solute on the activity of water and passivity breakdown**

476

477 In order to verify that the decrease of the activity of water is responsible for the decrease
478 of the susceptibility of Ti to undergo passivity breakdown in highly concentrated LiBr
479 solutions, additional electrolytes have been used to study the electrochemical behavior
480 of Ti. In the first case, the activity of water has been reduced by adding different
481 amounts of methanol to a 0.5M LiBr aqueous solution. a_W values in these solutions have
482 been estimated from literature [63] taking the values of a_W shown in **Table 1** as starting
483 point: water-free methanol solution ($a_W \approx 0$), 50 mol% water – 50 mol% methanol ($a_W \approx$
484 0.60) and 70 mol% water – 30 mol% methanol ($a_W \approx 0.76$). In the second case, the
485 activity of water has been increased by changing the bromide salt (LiBr was replaced by
486 KBr), since Li is the smallest alkali cation and it is most strongly hydrated, thus
487 reducing the amount of free water in the solution. A 3M KBr solution has been used,
488 whose molality m_{KBr} = 3.40 (mol KBr) (kg H_2O)$^{-1}$ is similar to that of a 3M LiBr
489 solution (m_{LiBr} = 3.77 (mol LiBr) (kg H_2O)$^{-1}$). The comparison of mean ionic activity
490 coefficients ($\gamma_\pm$) and activities of water (a_W) between LiBr and KBr solutions is shown
491 in **Figures 10a** and **10b**, respectively. It can be observed that $\gamma_\pm$ values are higher in
492 LiBr solutions than in KBr solutions in almost the whole range of molalities, while a_W
493 values are visibly lower for LiBr solutions than for KBr solutions at molalities higher
494 than 2 mol kg^{-1} (for 3M KBr and LiBr solutions, a_{W_KBr} = 0.89 and a_{W_LiBr} = 0.81).

495

496 **Figure 11** shows the potentiodynamic polarization curves of Ti in a 0.5M LiBr solution
497 with different water-methanol mol%. It can be observed that the four curves present a
498 clear passive range, regardless the water and methanol content. However, in the water-

free methanol solution, this passive range is significantly narrower than in the other solutions. Burstein and Whillock [64], as well as Banas et al [65], studied the passive behavior of Ti and other metals in methanolic solutions, and they concluded that methanol was responsible for the process of Ti dissolution, according to:

$$\mathrm{Ti} + n\mathrm{MeOH} \rightarrow \mathrm{Ti(OMe)}_{\mathrm{n}}^{(4-\mathrm{n})+} + n\mathrm{H}^{+} + 4\mathrm{e}^{-} \quad \textbf{(16)}$$

In the presence of water, (50 mol% water, 70 mol% water and aqueous solution), Ti presents considerably wider passive regions than in the free-water methanol solution (**Figure 11**). Apart from the formation of TiO_2 due to direct reaction of Ti with water molecules, the dissolved complex of Ti(IV) formed according to eq. (16) could hydrolyze to form additional TiO_2 [64]:

$$\mathrm{Ti(OMe)}_{\mathrm{n}}^{(4-\mathrm{n})+} + 2\mathrm{H_2O} \rightarrow \mathrm{TiO_2} + n\mathrm{MeOH} + (4-n)\mathrm{H}^{+} \quad \textbf{(17)}$$

It is clearly observed in **Figure 11** that the breakdown potential in the water-methanol mixed solutions is significantly higher than in the aqueous solution (E_{b70_30} = 4.9±0.2 V; E_{b50_50} = 3.7±0.3 V; $E_{b\_aqueous}$ = 2.6±0.2 V). This increase in E_b can be explained taking into account the decrease of free water in the electrolyte (i.e. decrease in a_W), by partially replacing the aqueous solvent by the methanolic one. Thus, although methanol causes Ti dissolution (eq. (16)), the decrease of a_W slows down the dissolution of the electrode surface via eqs. (12) and/or (15), in a similar way as in highly concentrated LiBr solutions.

The potentiodynamic polarization curves of Ti in 3M KBr and 3M LiBr solutions are presented in **Figure 12**. It can be observed that Ti is more susceptible to undergo passivity breakdown in the 3M KBr solution (E_{b_KBr} = 2.6±0.2 V) than in the 3M LiBr solution (E_{b_KBr} = 3.3±0.3 V). As it has been explained before, the mean ionic activity coefficient reaches higher values in LiBr than in KBr solutions due to the high charge density of the small lithium ion (**Figure 10a**). The higher activity coefficients in LiBr solutions result in higher activity of bromide anions (a_{Br^-} in the 3M KBr solution is 2.0 and a_{Br^-} in the 3M LiBr solution is 6.6). As stated in eq. (4), the value of E_b should be higher in the 3M KBr solution than in the 3M LiBr solution, since a_{Br^-} is significantly lower in the former electrolyte. However, the higher values of $\gamma_{\pm}$ in the LiBr solutions indicate a very strong interaction between water and ions, which lead to a decrease of a_W (**Figure 10b**). Again, the reduction of a_W in the 3M LiBr solution restricts the process of dissolution of the Ti surface (eqs. (12) and/or (15)), thus delaying the onset of stable passivity breakdown.

Relationship between E_b and a_W in concentrated LiBr solutions

The linear relationship with positive slope found between E_b and log a_{Br^-} in highly concentrated LiBr solutions (**Figure 3**) provides an empirical equation to evaluate E_b in function of the activity of bromide anions. However, according to the previous results, it is more coherent to relate E_b to the activity of water, a_W, since it is this parameter that directly affects the value of E_b in these concentrated media. Starting from eqs. (1) and (2), the activity of water can be expressed in terms of a_{Br^-}:

$$\log a_W = \frac{-\phi M_W \nu \frac{a_{Br^-}}{\gamma_\pm}}{2.303 \cdot 1000} = \frac{-\phi \cdot 18 \cdot 2 \frac{a_{Br^-}}{\gamma_\pm}}{2.303 \cdot 1000} = \frac{-A\phi a_{Br^-}}{\gamma_\pm} \quad \textbf{(18)}$$

On the other hand, a_{Br^-} can be expressed in terms of E_b by using the linear relationship E_b vs. log a_{Br^-} mentioned above (**Figure 3**):

$$a_{Br^-} = 10^{\frac{E_b - 2.50}{0.93}} \quad \textbf{(19)}$$

Substituting eq. (19) into eq. (18):

$$-\log a_W = \frac{A\phi}{\gamma_\pm} 10^{\frac{E_b - 2.50}{0.93}} \rightarrow \log(-\log(a_W)) = \log\left(\frac{A\phi}{\gamma_\pm}\right) + \left(\frac{E_b - 2.50}{0.93}\right)$$

Finally, solving for E_b yields:

$$E_b = 0.93 \cdot \left[\left(\log(-\log(a_W))\right) - \log\left(\frac{A\phi}{\gamma_\pm}\right) \right] + 2.50 \quad \textbf{(20)}$$

Eq. (20) relates the value of E_b to a logarithmic function of a_W. **Figure 13** shows the experimental and calculated values of E_b as a function of a_W in concentrated LiBr solutions. It can be observed that both experimental and calculated values of E_b are similar, indicating that eq. (20) can be used to satisfactorily calculate the breakdown potential of Ti in concentrated LiBr solutions (m_{LiBr} > ~ 0.7 mol kg^{-1}) as a function of the activity of water.

Finally, it is necessary to explain why Ti did not undergo passivity breakdwon in the 11.42M LiBr solution. According to eq. (20), the breakdown potential of Ti in the 11.42M LiBr solution (a_W = 0.12) should be 5.6 V. However, passivity breakdown was not observed even at potentials as high as 9 V. The absence of localized attacks in this solution can be explained by changes in the TiO_2 surface. The irreversible formation of titanium peroxo species at sufficiently high potentials (normally higher than $3V_{Ag/AgCl}$) has been reported in the literature [7, 8, 15]. The formation of Ti peroxo species may result in a very thin insulating or dielectric layer [8, 15] which would form in the hydrated (outer) part of the passive film above 3V [8]:

$$TiO_2 + OH^- \rightleftharpoons TiO_3 + H^+ + 2e^- \quad \textbf{(21)}$$

The presence of these species, such as TiO_3, can be noted by a yellowish color on the electrode surface [8]. This yellow color was observed on the undamaged areas of all the electrodes after the potentiodynamic polarization tests. However, the surface of the electrode polarized in the 11.42M LiBr solution had a dark golden color. The color-dependence of anodic Ti oxide layers on the polarization potential, and hence oxide thickness, is a very well known phenomenon [66-73]. For example, it has been observed [70, 71, 73] that at 5V the Ti surface has a light yellow color, while at 10-15V the surface color changes to dark golden/brown. Hence, the absence of stable localized attacks of Ti in the 11.42M LiBr solution can be attributed either to the formation of a highly insulating or dielectric layer of Ti peroxo species at potentials higher than ~5V (the value of E_p in the 8.06M LiBr solution is 4.7V) or/and to the increase of the Ti oxide film thickness. Both phenomena could block the interaction between aggressive anions and the surface of Ti, preventing passivity breakdown. This mechanism may be

similar to that reported by Sazou et al. [15] to explain passivity breakdown of Ti at high potentials in the presence of high concentrations of chlorides. In any case, it is evident that at sufficiently high potentials (higher than ~5V) the surface properties of the titanium oxide change to such an extent that the risk of passivity breakdown is completely eliminated, at least up to potentials as high as 9V.

5. CONCLUSIONS

A wide passive range where passive current density values (i_p) remained very low (of the order of 1-3 μA cm^{-2}) was observed in all LiBr solutions, indicating the excellent passive behavior of Ti. i_p values slightly increased with increasing LiBr concentrations up to 0.7M LiBr, where i_p started to decrease until reaching its lowest value (1 μA cm^{-2}) in the 11.42 LiBr solution.

In the low and moderately concentrated LiBr solutions, a decrease of E_b with increasing bromide concentrations was observed, while in the more concentrated LiBr solutions, E_b increased with increasing LiBr concentration. In the most concentrated LiBr solution (11.42M) Ti did not undergo passivity breakdown under the experimental conditions (up to 9 $V_{Ag/AgCl}$).

The steady-state passive current density, i_{SS}, was found to increase with Br^- concentration at relatively low concentrations, but it decreased at high LiBr concentrations, following the same tendency as i_p.

The passive film formed on Ti behaved as an *n*-type semiconductor, with the dominant defects in the passive film being oxygen vacancies and/or Ti^{3+} interstitials. An increase in LiBr concentration from 0.1M to 0.5M led to a clear increase of the donor density (N_D), but when increasing the LiBr concentration from 0.5M to 3M and 11.42M, N_D decreased. However, N_D values obtained in concentrated LiBr solutions were still higher than in the 0.1M LiBr solution, so the electronic properties of TiO_2 passive film could not be used to satisfactorily explain the increase of E_b at high LiBr concentrations or the absence of localized attacks in the 11.42M LiBr solution.

The resistance of the hydroxide outer layer of the passive film on Ti was higher in low concentrated LiBr solutions, whereas the resistance of the barrier layer of the film was found to be higher in concentrated LiBr solutions. These results could not be related to the degree of defectiveness of the passive film on Ti, but seemed to be associated with the passive film dissolution and the influence of the activity of water, a_W, on this process.

The activity of water, a_W, was found to have a strong influence on the susceptibility of Ti to undergo passivity breakdown. In view of the results, it may be concluded that a decrease in this parameter was responsible for the increase of the breakdown potential in highly concentrated LiBr solutions and water-methanol-LiBr mixtures. An empirical correlation between E_b and a_W was obtained for Ti in concentrated LiBr solutions.

ACKNOWLEDGEMENTS

We wish express our gratitude to the Ministerio de Ciencia e Innovación (Project CTQ2009-07518), and to Dr. M. Asunción Jaime for her translation assistance.

REFERENCES

[1] J. Been, J. S. Grauman, in: *Uhlig's Corrosion Handbook,* 2nd ed., R.Winston Revie (ed.), 863-885, Wiley Interscience, New York (2000).

[2] E. Blasco-Tamarit, A. Igual-Muñoz, J. García-Antón, D. García-García, Corros. Sci. **49**, 1000 (2007)

[3] Y. Z. Huang, D. J. Blackwood, Electrochim. Acta **51**, 1099 (2005)

[4] J. Pan, D. Thierry, C. Leygraf, Electrochim. Acta **41**, 1143 (1996)

[5] S. L. d. Assis, S. Wolynec, I. Costa, Electrochim. Acta **51**, 1815 (2006)

[6] J. R. Birch, T. D. Burleigh, Corrosion **56**, 1233 (2000)

[7] E. Peláez-Abellán, L. Rocha-Sousa, W. D. Müller, A. C. Guastaldi, Corros. Sci. **49**, 1645 (2007)

[8] K. Azumi, M. Seo, Corros. Sci. **43**, 533 (2001)

[9] V. A. Alves, R. Q. Reis, I. C. B. Santos, D. G. Souza, T. d. F. Gonçalves, M. A. Pereira-da-Silva, A. Rossi, L. A. da Silva, Corros. Sci. **51**, 2473 (2009)

[10] A. M. Schmidt, D. S. Azambuja, E. M. A. Martini, Corros. Sci. **48**, 2901 (2006)

[11] M. C. K. Sellers, E. G. Seebauer, Thin Solid Films **519**, 2103 (2011)

[12] Z. Jiang, X. Dai, H. Middleton, Mater. Chem. Phys. **126**, 859 (2011)

[13] D. S. Kong, W. H. Lu, Y. Y. Feng, Z. Y. Yu, J. X. Wu, W. J. Fan, H. Y. Liu, J. Electrochem. Soc. **156**, C39 (2009)

[14] B. Roh, D. D. Macdonald, Russ. J. Electrochem. **43**, 125 (2007)

[15] D. Sazou, K. Saltidou, M. Pagitsas, Electrochim. Acta **76**, 48 (2012)

[16] P. R. Roberge, *Handbook of Corrosion Engineering*, p. 756, McGraw-Hill, New York (2000).

[17] S. B. Basame, H. S. White, J. Phys . Chem. **99**, 16430 (1995)

672 [18] S. B. Basame, H. S. White, J. Electrochem. Soc. **147**, 1376 (2000)

673 [19] I. Dugdale, J. B. Cotton, Corros. Sci. **4**, 397 (1964)

674 [20] S. Virtanen, C. Curty, Corrosion **60**, 643 (2004)

675 [21] J. L. Trompette, L. Massot, L. Arurault, S. Fontorbes, Corros. Sci. **53**, 1262
676 (2011)

677 [22] N. Casillas, S. Charlebois, W. H. Smyrl, J. Electrochem. Soc. **141**, **636** (1994)

678 [23] T. R. Beck, J. Electrochem. Soc. **120**, 1310 (1973)

679 [24] S. Huo, X. Meng, Corros. Sci. **31**, 281 (1990)

680 [25] R. M. Fernández-Domene, E. Blasco-Tamarit, D. M. García-García, J. García-
681 Antón, Electrochim. Acta **58**, 264 (2011)

682 [26] P. Srikhirin, S. Aphornratana, S. Chungpaibulpatana, Renew. Sust. Energ.
683 Rev. **5**, 343 (2001)

684 [27] R. J. Lee, R. M. DiGuilio, S. M. Jeter, A. S. Teja, ASHRAE Tran. **96**, pt. 1
685 (1990)

686 [28] J. L. Guiñón, J. García-Antón, V. Pérez-Herranz, G. Lacoste, Corrosion **50**,
687 240 (1994)

688 [29] G. A. Florides, S. A. Kalogirou, S. A. Tassou, L. C. Wrobel, Energ. Convers.
689 Manage. **44**, 2483 (2003)

690 [30] R. D. Misra, P. K. Sahoo, A. Gupta, Int. J. Refrig. **28**, 331 (2005)

691 [31] W. J. Hamer, Y.-C. Wu, J. Phys. Chem. Ref. Data **1**, 1047 (1972)

692 [32] J. M. Prausnitz, R. N. Lichtenthaler, and E. G. Azevedo, *Molecular*
693 *Thermodynamics of Fluid-Phase Equilibria*, p. 517, Prentice Hall, Upper
694 Saddle River, NJ (1999).

695 [33] M. J. Blandamer, J. B. F. N. Engberts, P. T. Gleeson, J. C. R. Reis, Chem. Soc.
696 Rev. **34**, 440 (2005)

697 [34] H. Selcuk, J. J. Sene, M. V. Zanoni, H. Z. Sarikaya, M. A. Anderson,
698 Chemosphere **54**, 969 (2004)

699 [35] A. Igual-Muñoz, J. García-Antón, J. L. Guiñón, V. Pérez-Herranz,
700 CORROSION **59**, 606 (2003)

701 [36] M. J. Muñoz-Portero, J. García-Antón, J. L. Guiñón, R. Leiva-García, Corros.
702 Sci. **53**, 1440 (2011)

703 [37] A. D. Davydov, Electrochim. Acta **46**, 3777 (2001)

[38] L. F. Lin, C. Y. Chao, D. D. Macdonald, J. Electrochem. Soc. **128**, 1194 (1981)

[39] T. Haruna, D. D. Macdonald, J. Electrochem. Soc. **144**, 1574 (1997)

[40] D. D. Macdonald, J. Electrochem. Soc. **139**, 3434 (1992)

[41] D. D. Macdonald, Pure Appl. Chem. **71**, 951 (1999)

[42] D. D. Macdonald, Electrochim. Acta **56**, 1761 (2011)

[43] D. D. Macdonald, A. Sun, Electrochim. Acta **51**, 1767 (2006)

[44] K. Park, S. Ahn, H. Kwon, Electrochim. Acta **56**, 1662 (2011)

[45] D. D. Macdonald, J. Nucl. Mater. **379**, 24 (2008)

[46] A. D. Paola, Electrochim. Acta **34**, 203 (1989)

[47] W. P. Gomes, D. Vanmaekelbergh, Electrochim. Acta **41**, 967 (1996)

[48] M. Da Cunha Belo, N. E. Hakiki, M. G. S. Ferreira, Electrochim. Acta **44**, 2473 (1999)

[49] N. E. Hakiki, S. Boudin, B. Rondot, M. Da Cunha Belo, Corros. Sci. **37**, 1809 (1995)

[50] L. Hamadou, A. Kadri, N. Benbrahim, Appl. Surf. Sci. **252**, 1510 (2005)

[51] T. L. S. Wijesinghe, D. J. Blackwood, Corros. Sci. **50**, 23 (2008)

[52] J. Amri, T. Souier, B. Malki, B. Baroux, Corros. Sci. **50**, 431 (2008)

[53] D. G. Li, J. D. Wang, D. R. Chen, Electrochim. Acta **60**, 134 (2012)

[54] R. M. Fernández-Domene, E. Blasco-Tamarit, D. M. García-García, J. García-Antón, Electrochim. Acta **95**, 1 (2013)

[55] M. Urquidi-Macdonald, D. D. Macdonald, J. Electrochem. Soc. **136**, 961 (1989)

[56] A. M. Schmidt, D. S. Azambuja, Mater. Res. **9**, 387 (2006)

[57] G. J. Brug, A. L. G. van den Eeden, M. Sluyters-Rehbach, J. H. Sluyters, J. Electroanal. Chem. **176**, 275 (1984)

[58] C. Valero Vidal, A. Igual-Muñoz, Electrochim. Acta **55**, 8445 (2010)

[59] N. G. Smart, J. O. Bockris, Corrosion **48**, 277 (1992)

[60] G.S. Frankel, J. Electrochem. Soc. **145**, 2186 (1998)

[61] R. M. Fernández-Domene, E. Blasco-Tamarit, D. M. García-García, J. García-Antón, Int. J. Electrochem. Sc. **6**, 3292 (2011)

[62] E. Blasco-Tamarit, A. Igual-Muñoz, J. García-Antón, Corros. Sci. **49**, 4452 (2007)

[63] P. S. Crozier, R. L. Rowley, Fluid Phase Equilibr. **193**, 53 (2002)

[64] G. T. Burstein, G. O. H. Whillock, J. Electrochem. Soc. **136**, 1313 (1989)

[65] J. Banaś, B. Stypuła, K. Banaś, J. Światowska-Mrowiecka, M. Starowicz, U. Lelek-Borkowska, J. Solid State Electr. **13**, 1669 (2009).

[66] K.O. Beck, Titanium anodizing process, US Patent 2,949,411 (1960)

[67] J.L. Delplancke, M. Degrez, A. Fontana, R. Winand, Surf. Technol. **16**, 153 (1982)

[68] E. Gaul, J. Chem. Educ. **70**, 176 (1993)

[69] Y.T. Sul, C.B. Johansson, Y. Jeong, T. Albrektsson, Med. Eng. Phys. **23**, 329 (2001)

[70] Z. M. Yan, T. W. Guo, H. B. Pan, J. J. Yu, Mater. Trans. **43**, 3142 (2002)

[71] C. Chen, J. Chen, C. Chao, W.C. Say, J. Mater. Sci. **40**, 4053 (2005)

[72] M.V. Diamanti, B. Del Curto, M. Pedeferri, Color Res. Appl. **33**, 221 (2008)

[73] A. Karambakhsh, A. Afshar, S. Ghahramani, P. Malekinejad, J. Mater. Eng. Perform. **20**, 1690 (2011)

Tables

Table 1. Physical properties of the different LiBr solutions used in this work.

C_{LiBr}/mol l^{-1}	C_{LiBr}/g l^{-1}	m_{LiBr}/(mol LiBr) (kg H_2O)$^{-1}$	$\gamma_{\pm}$	a_{LiBr}	ϕ	a_W
0.05	4.34	0.05	0.93	0.05	0.95	1.00
0.10	8.68	0.10	0.80	0.08	0.94	1.00
0.30	26.05	0.31	0.76	0.23	0.95	0.99
0.50	43.42	0.51	0.75	0.39	0.97	0.98
0.70	60.79	0.72	0.77	0.56	1.00	0.97
1.15	100	1.20	0.84	1.01	1.07	0.95
3.00	260.52	3.77	1.75	6.60	1.53	0.81
4.61	400	5.69	3.56	20.26	1.93	0.67
8.06	700	11.18	21.89	222.82	2.95	0.34
11.42	992	15.15	154.00	2333.67	3.93	0.12

Table 2. Values of passive current density (i_p) at 0.4 V and breakdown potential (E_b) of Ti in different LiBr solutions, obtained from potentiodynamic polarization curves.

C_{LiBr}/mol l^{-1}	i_p/μA cm^{-2}	E_b vs (Ag/AgCl)/V
0.05	1.4 ± 0.1	3.8 ± 0.2
0.10	2.0 ± 0.2	3.2 ± 0.3
0.30	2.3 ± 0.2	2.7 ± 0.2
0.50	2.5 ± 0.3	2.6 ± 0.3
0.70	2.6 ± 0.1	2.2 ± 0.2
1.15	1.7 ± 0.1	2.7 ± 0.1
3.00	1.4 ± 0.1	3.3 ± 0.3
4.61	1.4 ± 0.1	3.8 ± 0.2
8.06	1.2 ± 0.1	4.7 ± 0.3
11.42	1.0 ± 0.2	-----

Table 3. Values of the equivalent circuit parameters for Ti in the 0.1M, 0.5M, 3M and 11.42M LiBr solutions.

C_{LiBr}/mol l^{-1}	R_S/Ω cm^2	R_1/kΩ cm^2	C_1/μF cm^{-2}	α_1	R_2/kΩ cm^2	C_2/μF cm^{-2}	α_2	χ^2 (x10^{-3})
0.1	7 ± 1	23 ± 3	3.8 ± 0.8	0.91 ± 0.01	2391 ± 157	4.6 ± 0.5	0.78 ± 0.24	0.9
0.5	4 ± 0	28 ± 2	4.4 ± 0.7	0.90 ± 0.01	1804 ± 116	10.5 ± 0.4	0.89 ± 0.14	1.8
3	1 ± 0	19 ± 2	3.4 ± 0.5	0.91 ± 0.01	3144 ± 108	1.3 ± 0.3	0.94 ± 0.09	3.5
11.42	2 ± 0	16 ± 2	3.2 ± 0.6	0.94 ± 0.01	3280 ± 101	3.9 ± 0.4	0.87 ± 0.07	4.1

Tables captions

Table 1. Physical properties of the different LiBr solutions used in this work.

Table 2. Values of passive current density (i_p) at 0.4 V and breakdown potential (E_b) of Ti in different LiBr solutions, obtained from potentiodynamic polarization curves.

Table 3. Values of the equivalent circuit parameters for Ti in the 0.1M, 0.5M, 3M and 11.42M LiBr solutions.

Figures captions

Fig. 1. Potentiodynamic polarization curves of Ti in different LiBr solutions at 25º C; (a) low and moderately concentrated LiBr solutions; (b) concentrated LiBr solutions.

Fig. 2. Images of the Ti electrode surface before and after the polarization tests in (a) 0.5M and (b) 11.42M LiBr solutions.

Fig. 3. Plots of E_b vs. log a_{Br^-} for Ti in the different LiBr solutions.

Fig. 4. Current density transients obtained after applying a potential step from a cathode value of -0.9 V to a passive value of 0.4 V for Ti in different LiBr solutions (0.1M, 0.5M, 3M and 11.42M).

Fig. 5. Capacitance-potential curves obtained for Ti in 0.5M LiBr solution at 0.4 V and at different frequencies.

Fig. 6. Mott-Schottky plots of the passive film formed on Ti in 0.1M, 0.5M, 3M and 11.42M LiBr solutions at 0.4 V, obtained at a frequency of 10 kHz.

Fig. 7. Values of donor density (N_D) of the passive film on Ti in different LiBr solutions (0.1M, 0.5M, 3M and 11.42M).

Fig. 8. Experimental and simulated Nyquist diagrams for Ti in 0.1M, 0.5M, 3M and 11.42M LiBr solutions at 0.4 V.

Fig. 9. Electrical equivalent circuit used to fit the experimental EIS data.

Fig. 10. Comparison of (a) mean ionic activity coefficients ($\gamma_{\pm}$) and (b) activities of water (a_W) between LiBr and KBr solutions.

Fig. 11. Potentiodynamic polarization curves of Ti in a 0.5M LiBr solution with different water-methanol mol%.

Fig. 12. Potentiodynamic polarization curves of Ti in 3M KBr and 3M LiBr solutions.

Fig. 13. Experimental and calculated (using eq. (20)) values of E_b as a function of a_W in the highly concentrated LiBr solutions.

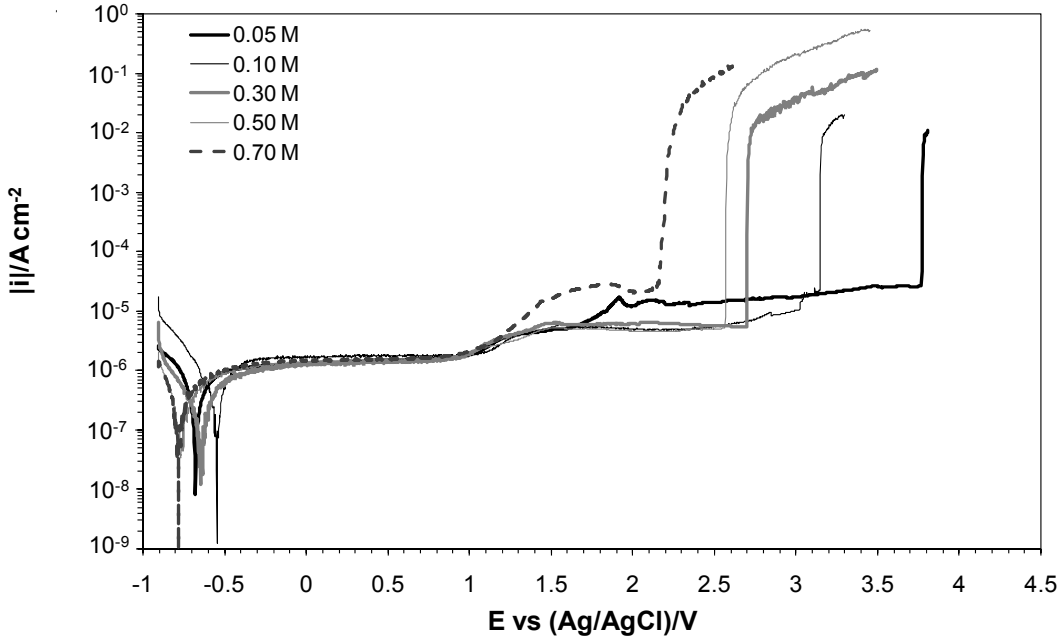
0.05 M
0.10 M
0.30 M
0.50 M
0.70 M
|i|/A cm-2
E vs (Ag/AgCl)/V

(a)

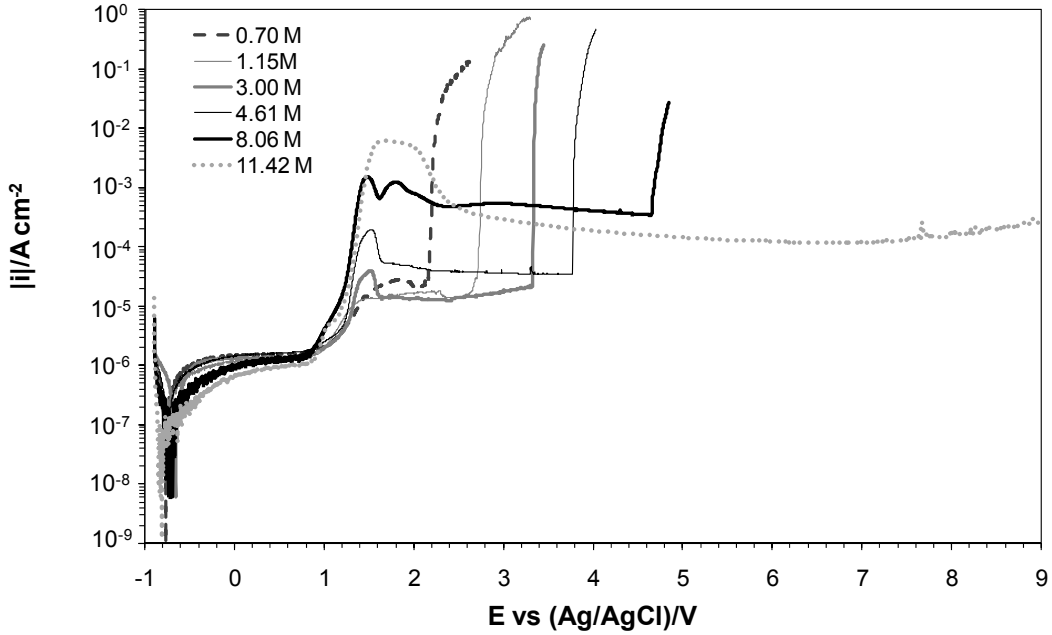
0.70 M
1.15M
3.00 M
4.61 M
8.06 M
11.42 M
|i|/A cm-2
E vs (Ag/AgCl)/V

(b)

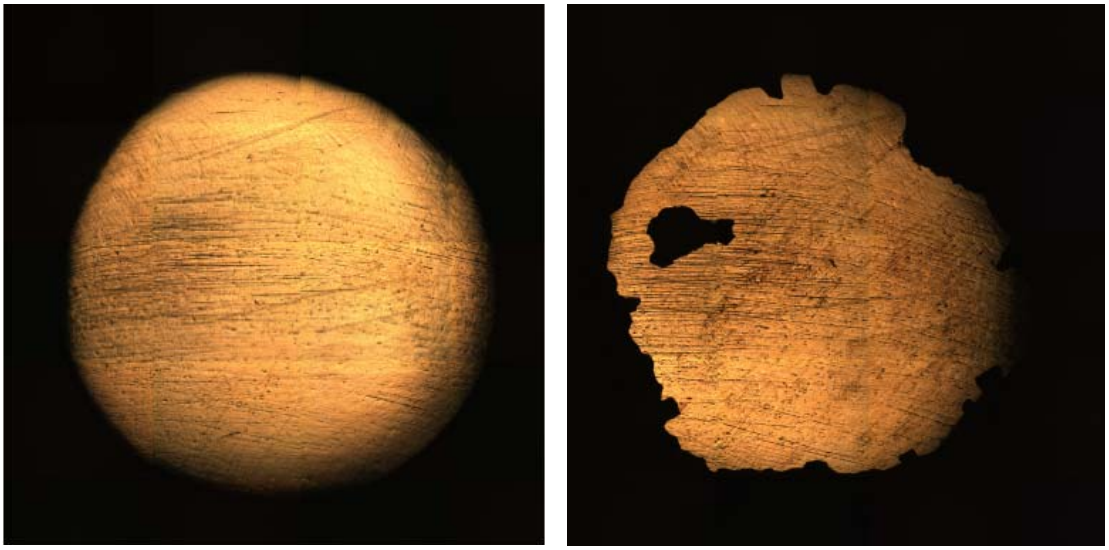

Initial mosaic (sample diameter = 8 mm) **Final mosaic (sample diameter = 8 mm)**

(a)

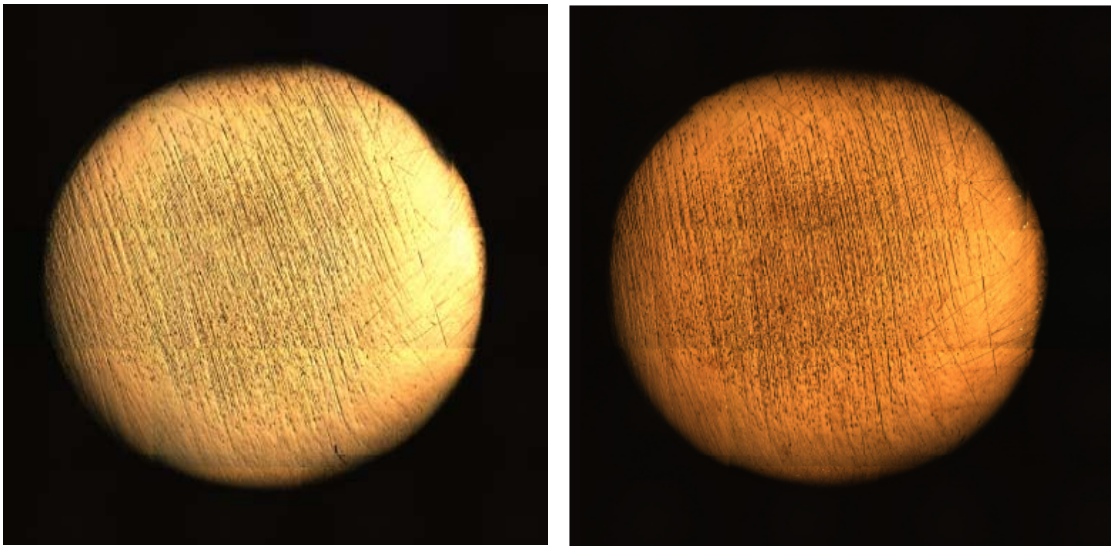

Initial mosaic (sample diameter = 8 mm) **Final mosaic (sample diameter = 8 mm)**

(b)

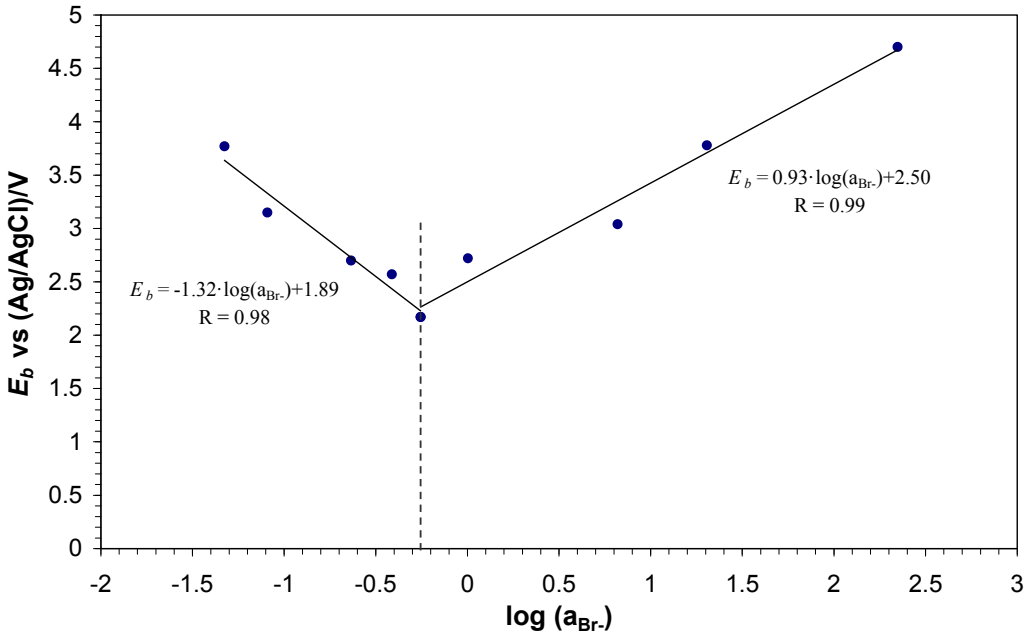
5
4.5
4
3.5
3
2.5
2
1.5
1
0.5
0
-2
-1.5
-1
-0.5
0
0.5
1
1.5
2
2.5
3
E_b vs (Ag/AgCl)/V
log (a_{Br^-})
E_b = -1.32·log(a_{Br^-})+1.89
R = 0.98
E_b = 0.93·log(a_{Br^-})+2.50
R = 0.99

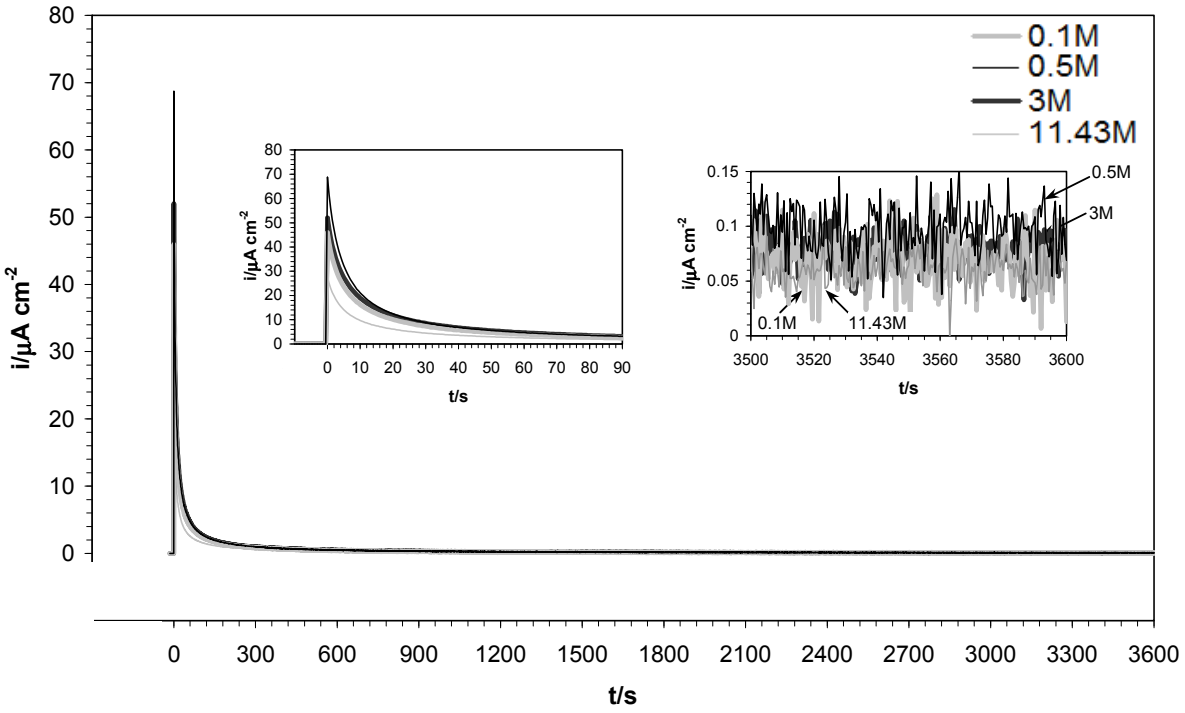
0.1M
0.5M
3M
11.43M
i/μA cm-2
t/s
0.5M
3M
0.1M
11.43M

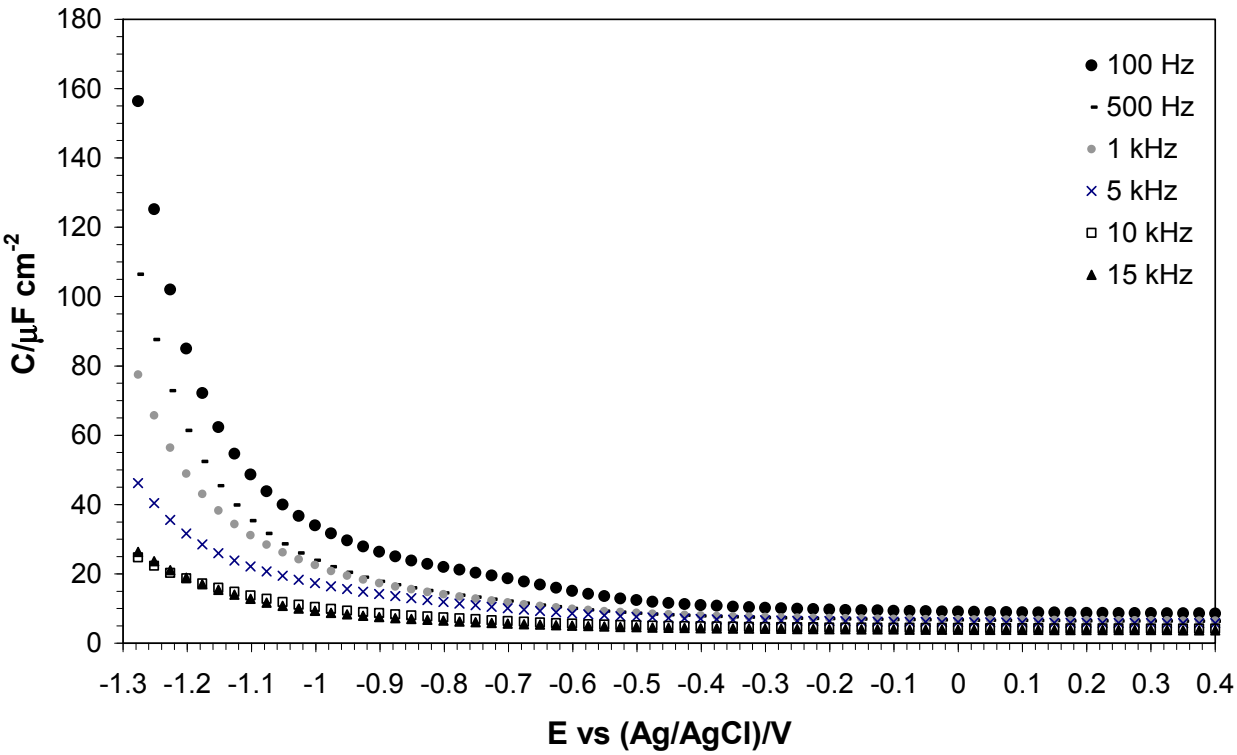
180
160
140
120
100
80
60
40
20
0
C/µF cm-2
-1.3 -1.2 -1.1 -1 -0.9 -0.8 -0.7 -0.6 -0.5 -0.4 -0.3 -0.2 -0.1 0 0.1 0.2 0.3 0.4
E vs (Ag/AgCl)/V
100 Hz
500 Hz
1 kHz
5 kHz
10 kHz
15 kHz

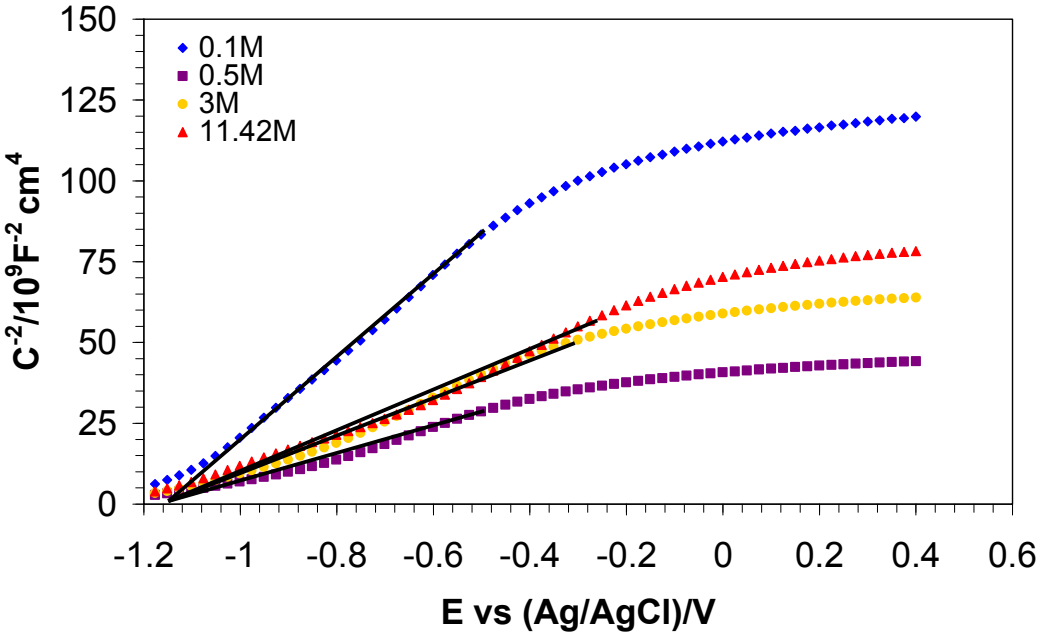
150
125
100
75
50
25
0
0.1M
0.5M
3M
11.42M
C-2/10^9F-2 cm4
-1.2
-1
-0.8
-0.6
-0.4
-0.2
0
0.2
0.4
0.6
E vs (Ag/AgCl)/V

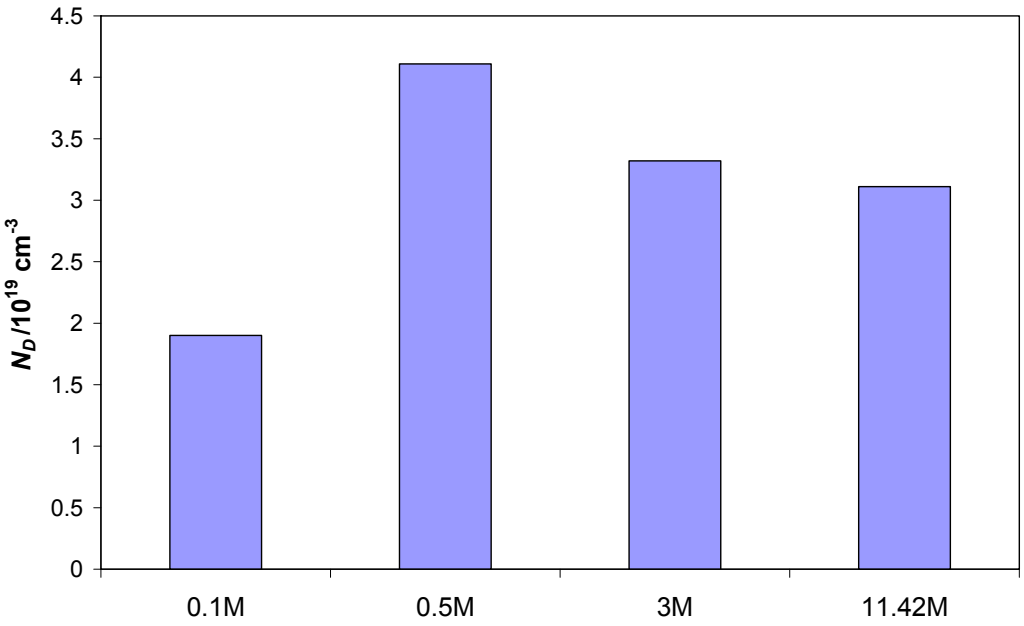
4.5
4
3.5
3
2.5
2
1.5
1
0.5
0
$N_D/10^{19}$ cm^{-3}
0.1M
0.5M
3M
11.42M

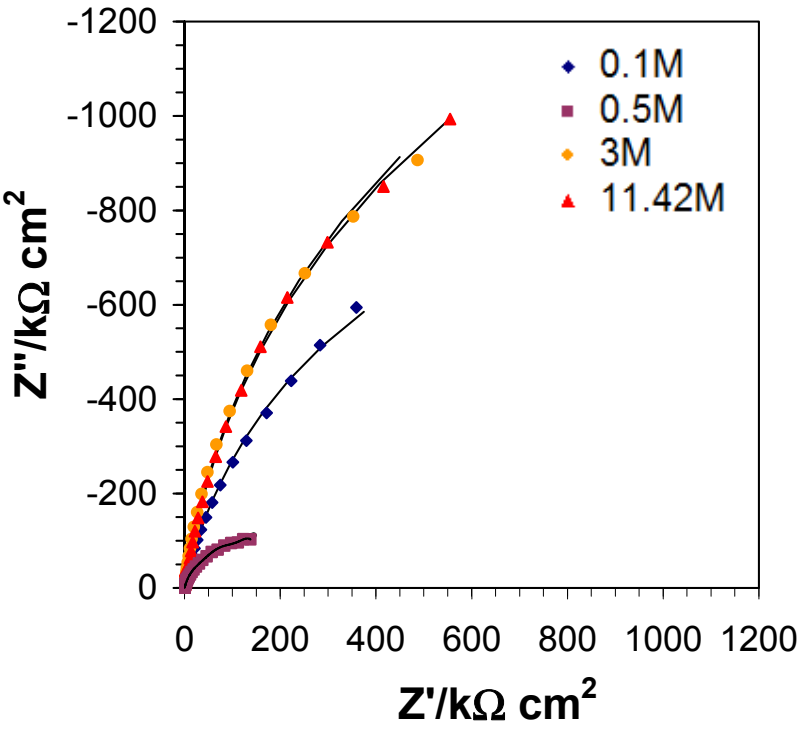
-1200
-1000
-800
-600
-400
-200
0
Z''/kΩ cm2
0
200
400
600
800
1000
1200
Z'/kΩ cm2
0.1M
0.5M
3M
11.42M

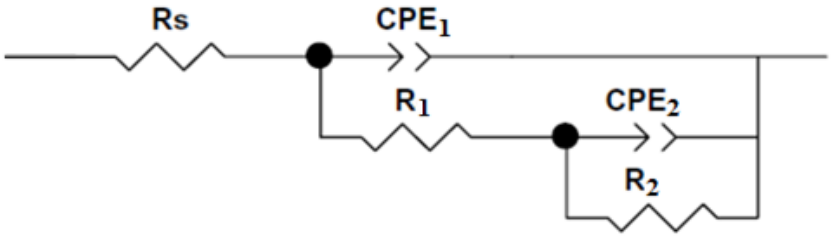
Rs
CPE1
R1
CPE2
R2

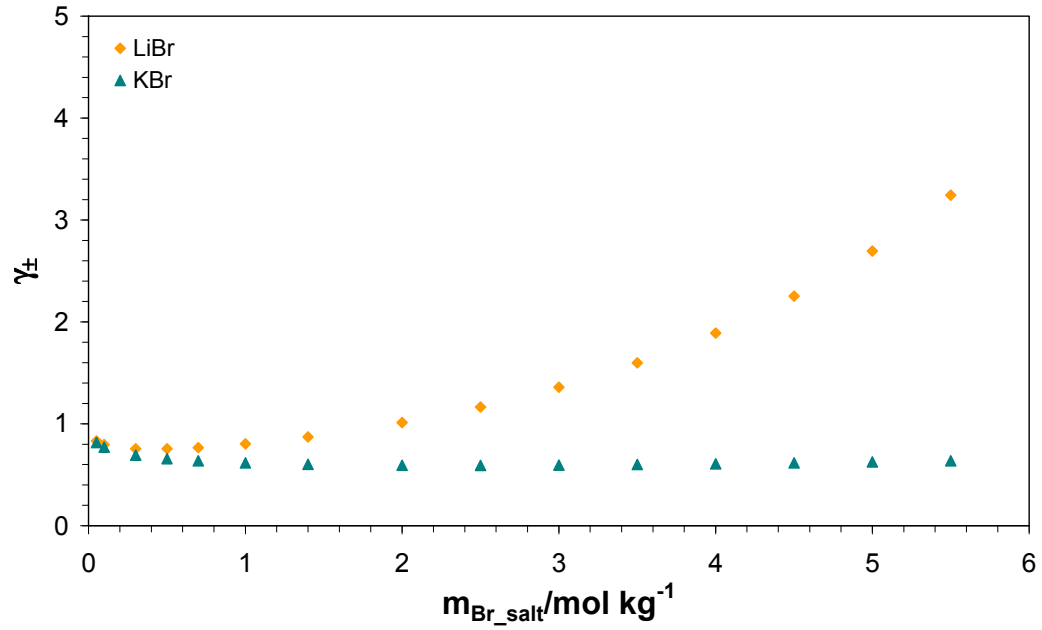

(a)

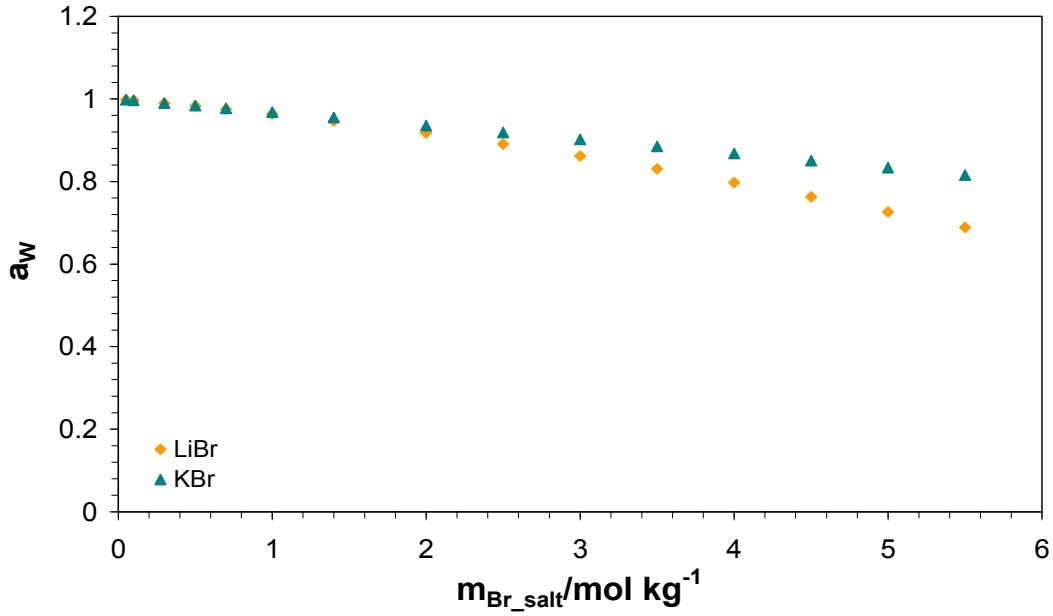

(b)

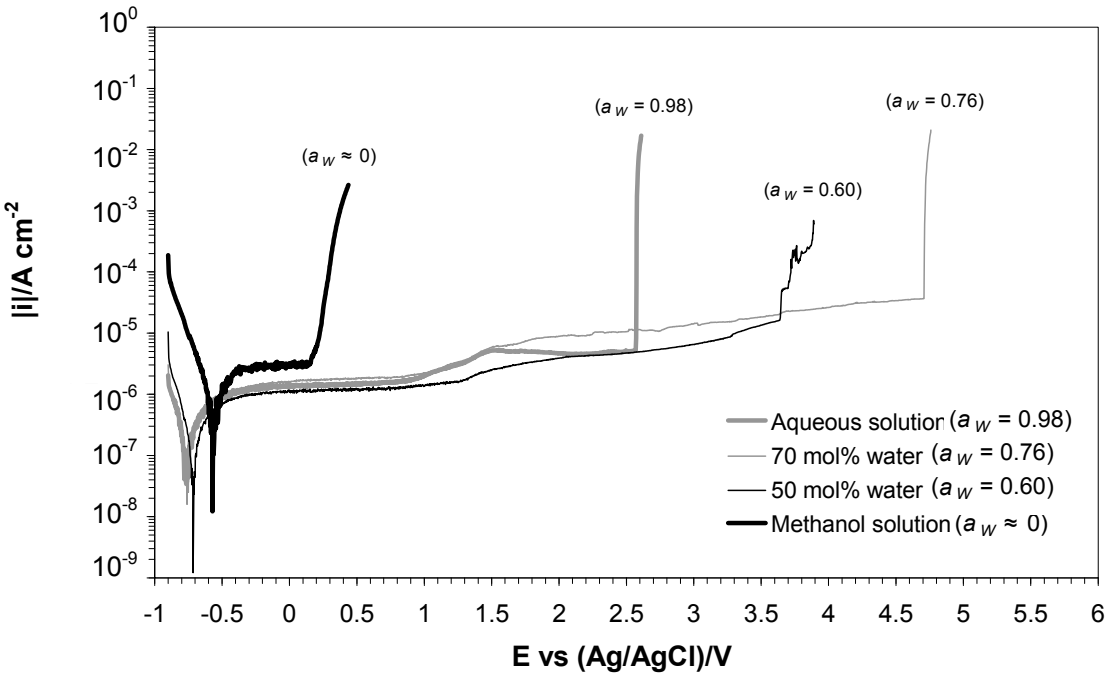
|i|/A cm-2
E vs (Ag/AgCl)/V
(a W = 0.98)
(a W = 0.76)
(a W ≈ 0)
(a W = 0.60)
Aqueous solution (a W = 0.98)
70 mol% water (a W = 0.76)
50 mol% water (a W = 0.60)
Methanol solution (a W ≈ 0)

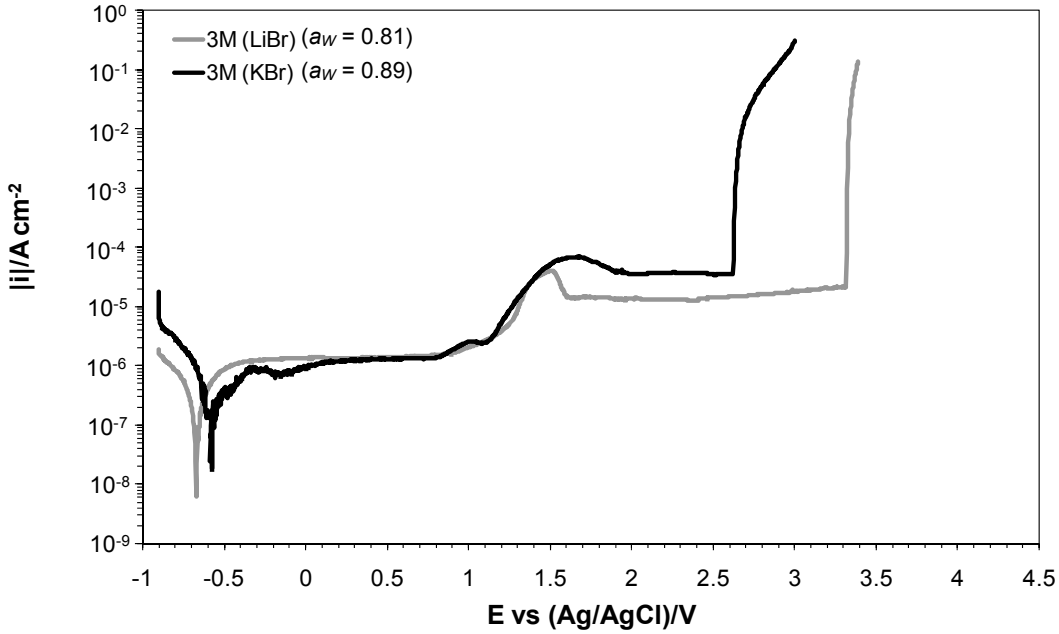
3M (LiBr) (a_W = 0.81)
3M (KBr) (a_W = 0.89)
|i|/A cm-2
E vs (Ag/AgCl)/V

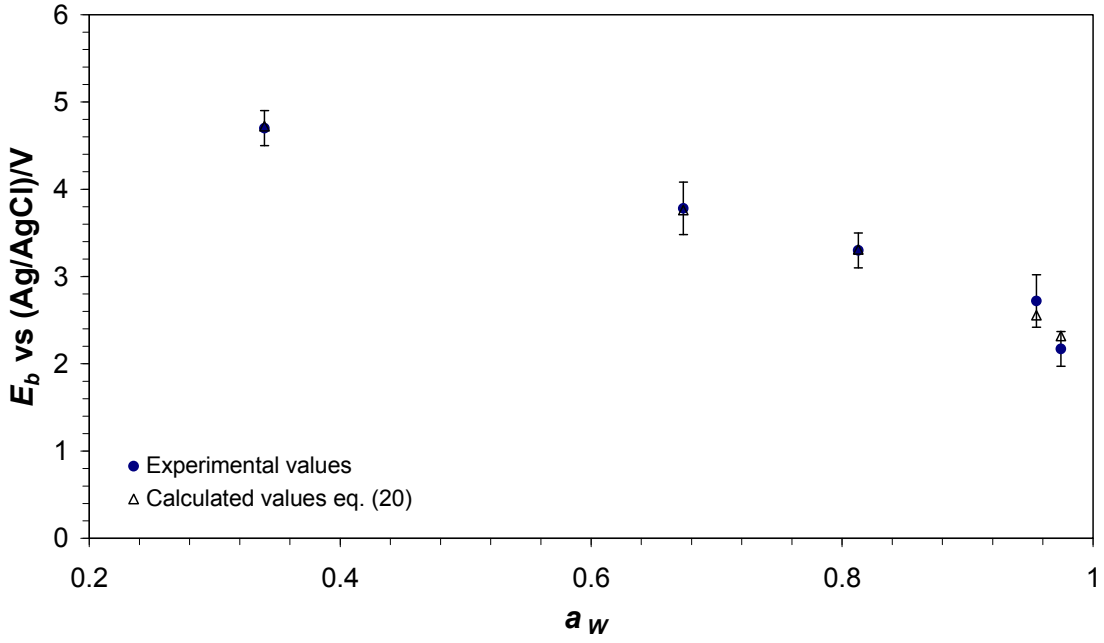
6
5
4
3
2
1
0
0.2
0.4
0.6
0.8
1
E_b vs (Ag/AgCl)/V
a_w
Experimental values
Calculated values eq. (20)